

Analogue of the Quantum Hanle Effect and Polarization Conversion in Non-Hermitian Plasmonic Metamaterials

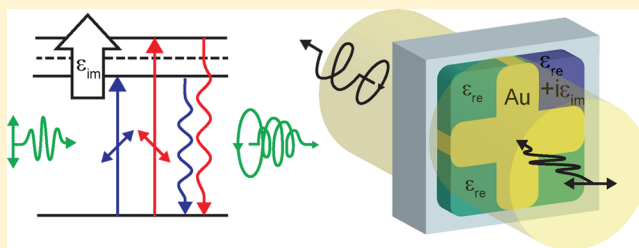
Pavel Ginzburg,^{*,†,§} Francisco J. Rodríguez-Fortuño,^{†,‡,§} Alejandro Martínez,[‡] and Anatoly V. Zayats[†]

[†]Department of Physics, King's College London, Strand, London WC2R 2LS, United Kingdom

[‡]Nanophotonics Technology Center, Universitat Politècnica de València, 46022 Valencia, Spain

ABSTRACT: The Hanle effect, one of the first manifestations of quantum theory introducing the concept of coherent superposition between pure states, plays a key role in numerous aspects of science varying from applicative spectroscopy to fundamental astrophysical investigations. Optical analogues of quantum effects help to achieve deeper understanding of quantum phenomena and, in turn, to develop cross-disciplinary approaches to realizations of new applications in photonics. Here we show that metallic nanostructures can be designed to exhibit a plasmonic analogue of the quantum Hanle effect and the associated polarization rotation. In the original Hanle effect, time-reversal symmetry is broken by a static magnetic field. We achieve this by introducing dissipative level crossing of localized surface plasmons due to nonuniform losses, designed using a non-Hermitian formulation of quantum mechanics. Such artificial plasmonic “atoms” have been shown to exhibit strong circular birefringence and circular dichroism which depends on the value of loss or gain in the metal-dielectric nanostructure.

KEYWORDS: Plasmonics, metamaterials, nanoparticles, polarization conversion



The quantum Hanle effect describes the polarization rotation of scattered electromagnetic radiation due to atomic coherence between Zeeman states split by a magnetic field.¹ This is a key phenomenon in high-resolution atom spectroscopy,² detection of magnetic fields in solar prominence³ and stellar winds.⁴ The main advantage in these measurements is a very high spectral resolution provided by the Hanle effect since the level crossing is not limited by the Doppler width of the spectral lines but solely by the coherence of the states in individual atoms, and sensitivity to magnetic fields. The observation of the effect is possible in the presence of a magnetic field which violates the time-reversal symmetry as was observed in the experiments on coherent backscattering⁵ and can contribute to parity symmetry breaking.⁶

The investigations of optical analogues of quantum effects are important to achieve deeper understanding of quantum phenomena and give prospect to new applications based on cross-disciplinary approaches. For example, the realization of sharp spectral resonances with metallic (plasmonic) nanostructures important for biosensing and nonlinear photonic applications has resulted from the studies of optical counterparts of the Fano resonance, relying on the interference between scattering amplitudes of bound and continuum electronic states,⁷ and electromagnetically induced transparency (EIT) due to destructive interference of electron probability amplitudes induced by two spectrally different optical beams.⁸

In this Letter, we investigate an optical counterpart of the quantum Hanle effect. By employing the concepts of non-Hermitian quantum mechanics,^{9,10} we have designed an artificial plasmonic “atom” which has a pair of degenerate

resonances that split by broken time-reversal symmetry due to the presence of loss. This is a complete optical analogue of the atomic system where initially degenerate atomic states are split when the time-reversal symmetry is broken by a magnetic field.¹ The removal of degeneracy of the plasmonic resonances leads to very strong birefringence and circular dichroism, again in analogy with the quantum Hanle effect in atomic systems.

The basic scheme of the Hanle effect is represented in Figure 1a,b. Linearly polarized light, being a superposition of left and right circular polarizations, coherently excites the p-orbitals of an atom, conserving the total angular momentum. The degeneracy between p-states (Figure 1a) could be removed by an applied static magnetic field (Figure 1b). The excited p-states decay in time with slightly dissimilar time constants, adding different phases for opposite circular polarizations and, as a consequence, resulting in polarization-unpreserved light scattering. The polarization of the scattered light depends then on the strength of the magnetic field which determines the splitting between states.

The plasmonic “atom level” diagram of our optical analogue is shown in Figure 1c,d. We have considered a plasmonic “atom” which can be a metal nanoparticle with two localized surface plasmon (LSP) resonances. These resonances, in the quasistatic approximation valid for small nanoparticles, are solely determined by the particle’s shape and surrounding environment and can be engineered and tuned to the desired

Received: September 13, 2012

Revised: November 12, 2012

Published: November 19, 2012

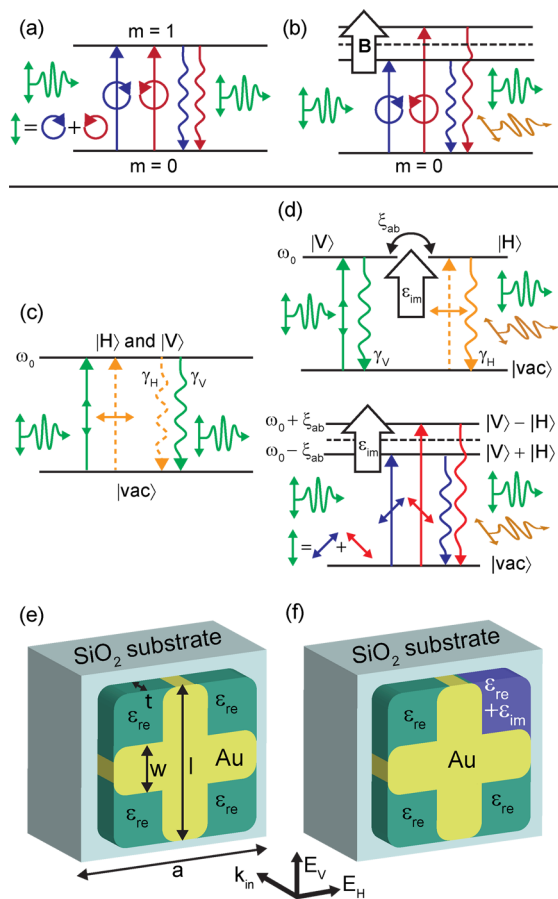


Figure 1. Quantum Hanle effect and its plasmonic analogue. (a, b) Basic level structure of “traditional” Hanle effect (a) without and (b) with an applied magnetic field to break time-reversal symmetry. (c, d) Optical counterpart of the Hanle effect in an artificial plasmonic atom: (c) Degenerate LSP resonances in the symmetric particle and (d) loss-induced coupling of the resonances $|H\rangle$ and $|V\rangle$ (top) and its equivalent scenario of the splitting into two supermodes $|V\rangle+|H\rangle$ and $|V\rangle-|H\rangle$ (bottom). (e, f) Schematics of the plasmonic metamaterial for the observation of the Hanle effect analogue: (e) a metal nanocross in a uniform embedding dielectric with degenerate LSP resonances, (f) one quadrant of the embedding dielectric is lossy leading to the splitting of LSP resonances of the otherwise symmetric metallic nanostructure.

frequency.^{11–13} The vacuum state $|vac\rangle$ (no LSPs excited) represents the ground state of an atom. The degenerate in frequency LSP resonances corresponding to the excitation with different polarizations of the incident light are the analogues of the p-orbitals of the atom (marked as $|H\rangle$ and $|V\rangle$ on the diagram (Figure 1c) for horizontal and vertical polarizations, respectively). The degeneracy of these LSP states can be removed by dissipative coupling in the presence of nonuniform loss (Figure 1d), resulting in the shift of LSP resonances with respect to each other, as will be shown below.

The nanoparticle analyzed in this work has been considered to be a metallic cross that has two degenerate dipolar LSP resonances corresponding to horizontal ($|H\rangle$) and vertical ($|V\rangle$) polarizations, respectively (Figure 1e). This particle represents the above description if embedded in a uniform dielectric. In this degenerate case, the polarization of the light normally incident on the nanostructure will not change upon reflection or in transmission. In principle, degeneracy may take place between plasmonic resonances of any order and could

lead to interesting effects due to their interplay and time evolution.¹⁴

The degeneracy between the LSP resonances can be removed by introduction of losses ($\epsilon_{im} \neq 0$) in some locations near the cross arms (Figure 1f). In this situation, the $|H\rangle$ and $|V\rangle$ modes of the particle are coupled, giving rise to the uncoupled $|H\rangle+|V\rangle$ and $|H\rangle-|V\rangle$ modes excited by light with two orthogonal polarizations oriented at 45° to the cross arms. These polarizations are always preserved after interaction with the structure due to its symmetry. Except for these light polarizations, such plasmonic nanoparticle with coupled $|H\rangle$ and $|V\rangle$ LSP states coherently scatters a fraction of the linearly polarized light into the orthogonal polarization state, leading to elliptization of linearly or circularly polarized incident light. Thus, the polarization of the reflected/transmitted light will depend on the splitting of the LSP resonances governed by the loss—in analogy to the modification of the polarization state of light scattered by atoms in the quantum Hanle effect depending on the splitting of atomic levels governed by magnetic field.

To analyze the loss-induced interplay and coupling between eigenmodes of the structure, we developed a rigorous theoretical description using the non-Hermitian quantum mechanical approach to describe loss-induced coupling between LSP resonances.^{9,10} Non-Hermitian formulation of quantum mechanics is especially useful in the description of dissipative systems helping to get rid of ‘bath’ degrees of freedom. This formulation arises from the fact that probability conservation does not necessarily mean the hermiticity of time-evolution operators, but just the combination of parity and time-reversal commutations with an appropriate Hamiltonian of the system. Several interesting optical phenomena, such as higher harmonics generation¹⁵ or unidirectional mode coupling in waveguide structures,¹⁶ have been analyzed in terms of this non-Hermitian formalism. For the plasmonic system under consideration, the eigenmodes can be derived from the solution of the following master equations:¹⁷

$$\Theta(\vec{H}(\vec{r})) = \left(\frac{\omega}{c}\right)^2 \vec{H}(\vec{r})$$

$$\Theta(\vec{H}(\vec{r})) = \nabla \times \left[\frac{1}{\epsilon(\vec{r}, \omega)} \nabla \times \vec{H}(\vec{r}) \right] \quad (1)$$

where $\vec{H}(\vec{r})$ is the magnetic field of the mode, ω is the angular frequency, c is the speed of light in vacuum, and $\epsilon(\vec{r}, \omega)$ is the position- and frequency-dependent dielectric constant. If both dispersion and absorption of the medium are neglected, the above-defined Θ -operator is Hermitian and forms a complete orthogonal set of eigenmodes $\{\vec{H}(\vec{r})\}$. Nevertheless, for certain problems, such as lasers, optical amplifiers, or lossy structures, even if a single frequency is considered, the dielectric permittivity is a complex number, and the Θ -operator is not Hermitian anymore. Nevertheless, it is always possible to decompose it into a sum of the Hermitian and anti-Hermitian parts as follows:

$$\Theta(\vec{H}(\vec{r})) = \Theta_H(\vec{H}(\vec{r})) + \Theta_A(\vec{H}(\vec{r}))$$

$$\Theta_H(\vec{H}(\vec{r})) = \nabla \times \left[\frac{\epsilon_r(\vec{r}, \omega)}{\epsilon_r^2(\vec{r}, \omega) + \epsilon_{im}^2(\vec{r}, \omega)} \nabla \times \vec{H}(\vec{r}) \right]$$

$$\Theta_A(\vec{H}(\vec{r})) = -i \nabla \times \left[\frac{\epsilon_{im}(\vec{r}, \omega)}{\epsilon_r^2(\vec{r}, \omega) + \epsilon_{im}^2(\vec{r}, \omega)} \nabla \times \vec{H}(\vec{r}) \right] \quad (2)$$

where Θ_H and Θ_A are the Hermitian and anti-Hermitian operators and $\epsilon(\vec{r}, \omega) = \epsilon_r(\vec{r}, \omega) + i\epsilon_{im}(\vec{r}, \omega)$. Θ_H provides an orthogonal set of eigenmodes spanning the entire electromagnetic space.

In the following, we have considered only two modes $|a\rangle$ and $|b\rangle$ and investigated their coupling originating from the presence of loss or gain ($\Theta_A \neq 0$). The total magnetic field is given by the sum of the individual modes:

$$\vec{H}(\vec{r}) = a(t)\vec{H}_a(\vec{r})e^{i\omega t} + b(t)\vec{H}_b(\vec{r})e^{i\omega t} \quad (3)$$

where $a(t)$ and $b(t)$ are the complex time-dependent amplitudes of each mode. In the case of small imaginary part of the permittivity ($\epsilon_r(\vec{r}, \omega) \gg \epsilon_{im}(\vec{r}, \omega)$), the time evolution can be obtained in the slowly varying amplitudes ($a(t), b(t)$) approximation by inserting eq 3 into eq 2 and taking into account the orthogonality of the field components ($\int \vec{H}_i^*(\vec{r}) \cdot \vec{H}_j(\vec{r}) d^3\vec{r} = (\hbar\omega/2\mu_0)\delta_{ij}$) as

$$\frac{da(t)}{dt} = -\xi_a a(t) - \xi_{ab} b(t)$$

$$\xi_a = \frac{\epsilon_0}{\hbar} \int \epsilon_{im}(\vec{r}) \vec{E}_a^*(\vec{r}) \vec{E}_a(\vec{r}) d^3\vec{r}$$

$$\xi_{ab} = \frac{\epsilon_0}{\hbar} \int \epsilon_{im}(\vec{r}) \vec{E}_a^*(\vec{r}) \vec{E}_b(\vec{r}) d^3\vec{r} \quad (4)$$

where $\vec{E}_j(\vec{r})$ is the electric field corresponding to the j -th mode and \hbar is the reduced Planck constant, and μ_0 and ϵ_0 are the permeability and permittivity of free space. A similar equation may be obtained for the amplitude of the mode $b(t)$.

As can be seen from eq 4, the coupling between the two modes is determined by an overlap integral weighted by the position-dependent imaginary part of the permittivity. For symmetric structures with uniform losses, the coupling coefficients between two modes will be identically zero. However, the situation will be completely different if the medium is not uniformly lossy (e.g., selectively doped dielectric substrate or electrically or optically induced loss or gain). The loss-induced coupling will cause the removal of the degeneracy and will lead to the modification of the polarization state of scattered light (Figure 1d).

The transmission spectra of the structure were modeled as described in Methods. For the polarization of the incident light corresponding to the states $|H\rangle+|V\rangle$ and $|H\rangle-|V\rangle$ which remains unchanged after interaction with the nanostructure, a single transmission minimum is observed in the absence of loss related to the excitation of the degenerate LSP modes associated with the cross-arms (Figure 2). The characteristic field distribution near the plasmonic nanoparticle corresponds to the simultaneous excitation of two dipolar antennas.

When nonuniform losses are included, the states $|H\rangle+|V\rangle$ and $|H\rangle-|V\rangle$ become nondegenerate with the splitting increasing with the loss, and their field distribution is distinctly different (Figure 2): one is symmetric due to the symmetry of

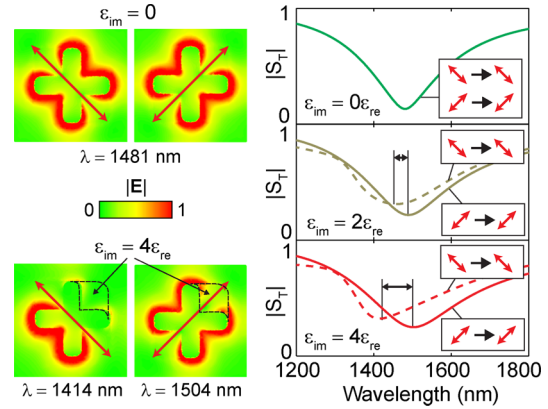


Figure 2. Removing degeneracy of LSP modes due to dissipative coupling. The spectra of transmission scattering parameters showing the absorption of the modes $|H\rangle+|V\rangle$ and $|H\rangle-|V\rangle$ of the nanocross (Figure 1f). The polarization state of the modes cannot be modified by the nanostructure without nonuniform loss. The splitting of the degenerate LSP resonances is observed with the increase of the nonuniform loss in the dielectric. The electric field distribution in the nanostructure for degenerate and split resonances are shown next to the spectra. The parameters of the plasmonic structure marked in Figure 1e were taken to be $w = 100$ nm, $t = 20$ nm, and $l = 400$ nm. For other parameters of the calculations see Methods.

the structure while the second one is antisymmetric with the field concentrated over the region with smaller loss. At the same time for linear polarizations $|V\rangle$ and $|H\rangle$ (Figure 3a), the absorption resonance exhibits broadening and becomes asymmetric with the hint of the presence of two resonances (these can only be resolved in differential spectra). The fact

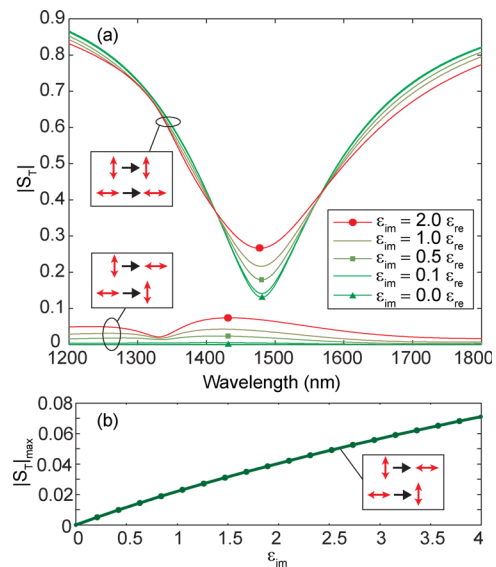


Figure 3. Polarization conversion due to the Hanle effect. (a) Spectral dependence of the scattering parameters S_T near the LSP resonance for different values of nonuniform loss. The upper set of curves correspond to the transmission of linearly polarized light ($|H\rangle$ or $|V\rangle$) and is related to the absorption without polarization changes. The lower set of curves shows polarization conversion efficiency defined as the scattering parameter from one linear polarization ($|H\rangle$ or $|V\rangle$) state into the orthogonal polarization state. (b) Dependence of the polarization conversion efficiency on the coupling loss. The parameters of the plasmonic structure are the same as in Figure 2.

that the two separate peaks are not clearly resolved in the transmission simulations for $|V\rangle$ and $|H\rangle$ is in agreement with the theoretical predictions. The width of the resonances is determined by the coefficients ξ_a and ξ_b (eq 4) which depend on both metal and dielectric losses, while the level splitting is defined by the coupling coefficient ξ_{ab} . Assuming a nonuniformly lossy dielectric environment ($\epsilon_{im}(\vec{r}) > 0$), the weighted Hermitian inner product over L^2 metric space may be defined, and the Cauchy–Schwarz inequality will hold $\xi_a \xi_b \geq |\xi_{ab}|^2$. This implies that in this system the broadening of the resonances with the loss increase will always be greater than the splitting, preventing the direct observation of the splitting of the resonances. This is in striking contrast with the plasmonic analogues of EIT, where the splitting is larger than the resonance width.⁸ In our case the coupling takes place between two “bright” modes, while a “dark” (with narrow line width) mode is generally used for EIT.

The strong influence of such nanostructures on the polarization properties of light is expected as in the traditional Hanle effect due to the interplay of the resonances which respond differently to different incident light polarizations. The lower set of curves in Figure 3a show the scattering efficiency of the input linear E_V or E_H polarization into the orthogonal polarization. This cross-polarization scattering leads to elliptization of the incident linear polarized light upon reflection and in transmission. The overall conversion efficiency reaches 10% in the vicinity of the resonance in just a 20 nm thick layer of metamaterial and may be improved by increasing losses (Figure 3b).

The steady state behavior of the system may be analyzed in terms of “rate equations” following the energy diagram in Figure 1d. The mode population of the vertical ($|V\rangle$) resonance under the incident E_H (H-polarized) field can be obtained as

$$V = \frac{\xi_{ba}(\gamma_{V,\text{rad}} + \gamma_{V,\text{dis}})(\gamma_{H,\text{rad}} + \gamma_{H,\text{dis}})}{\xi_{ba}\xi_{ab}(\gamma_{V,\text{rad}} + \gamma_{V,\text{dis}})(\gamma_{H,\text{rad}} + \gamma_{H,\text{dis}}) - 1} \kappa E_H$$

$$\approx -\kappa \xi_{ba}(\gamma_{V,\text{rad}} + \gamma_{V,\text{dis}})(\gamma_{H,\text{rad}} + \gamma_{H,\text{dis}}) E_H \quad (5)$$

where E_H is the input “H”-polarized field amplitude, κ is the excitation efficiency of the $|H\rangle$ resonance under E_H illumination, and $\gamma_{V,\text{rad}}$ and $\gamma_{V,\text{dis}}$ are the radiative and nonradiative (dissipative) lifetimes of the resonance, respectively. In the approximation made in eq 5, we have assumed that the coupling ξ_{ab} is small compared to the damping coefficient which is proportional to ξ_a and ξ_b (eq 4). The far-field intensity of light with the rotated polarization is proportional to $V/\gamma_{V,\text{rad}}$. The behavior of the conversion efficiency with ξ_{ab} , predicted to be linear by eq 5, is verified by the numerical experiment for small losses where eq 5 is valid, and deviates slightly from linear dependence for larger losses (Figure 3b).

Finally, we have considered the effect of this structure on incident circularly polarized light. The amplitude ratio and the phase difference between the vertical and horizontal components transmitted through and reflected from the structure for left and right circular polarizations show that light experiences significant elliptization, different for different handedness of the incident light (Figure 4). The degree of elliptization also depends on how close the wavelength of the incident light is to the plasmonic resonances and on the loss.

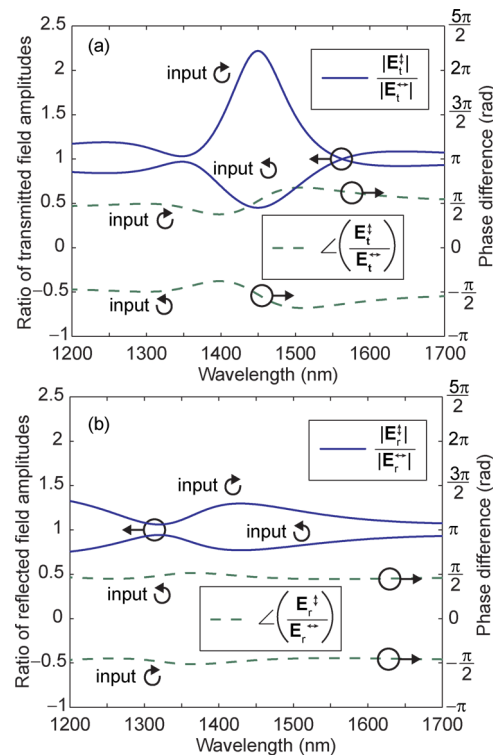


Figure 4. Circular dichroism in the non-Hermitian plasmonic metamaterial. Amplitude ratio (solid line) and phase difference (dashed line) of the E_V and E_H field components for (a) transmitted and (b) reflected light when the normally incident plane wave is right or left circularly polarized. The parameters of the plasmonic structure are the same as in Figure 2.

In conclusion, we have introduced an analogue of the quantum Hanle effect in artificial plasmonic atoms. Ordered arrays of such plasmonic “atoms” have shown to form a metamaterial with extraordinarily pronounced circular birefringence and circular dichroism induced by the loss-coupled LSP states. The efficient control of the polarization state of light can be achieved using this effect in deep-subwavelength thick slabs (20 nm thickness) in both reflection and transmission geometries.

Possible experimental tests of the proposed concept can be realized using lithographically defined plasmonic nanocrosses or, in complementary geometry, cross-shaped apertures in a metal (plasmonic) film. The use of low-loss plasmonic material will be advantageous to provide highest possible differential contrast with the additional loss needed for coupling. The required spatially nonuniform losses can be implemented with selective doping of semiconductor coating,¹⁸ selective polymerization of the monomer cover layer,¹⁹ or indeed controlled dynamically using electric-field, temperature, or light-induced absorption.

Polarization manipulation by 2D optically active artificially structured media has been previously demonstrated in several configurations, such as planar arrays of subwavelength gammadions,²⁰ plasmonic crystals,^{21,22} spiral bull-eye structures,²³ and 3D metamaterials.^{24–27} The use of the loss-coupled states open up the possibility to build metamaterial components for active control of the reflected or transmitted light polarization if the nonuniform loss can be selectively induced by external stimuli, such as thermal, electric, or optical signals. The optical response of the coupled nanocrosses

resembles the response of nanoantennas recently used to achieve phase control and, thus, the control of refraction and reflection from the material interface structured in this way;^{28,29} therefore, active manipulation of loss-induced coupling may help to achieve active control over phase of reflected/transmitted light. If turned around, the effect can be used for measurements of local absorption (or gain) in metamaterials via polarization measurements or indeed in sensing applications³⁰ for analytes introducing optical loss. Understanding spatially nonuniform loss/gain coupling is also imperative for the development of loss-compensation and gain in metamaterials, where loss may result in additional and sometimes undesirable effects. From the fundamental point of view, the proposed general formalism for dissipative level crossing by employing the non-Hermitian effects in metamaterials may be used to analyze and design new effects in plasmonic systems where metal loss is intrinsically present.

Methods. To validate the analytical results, we have numerically simulated gold nanocrosses on a silica substrate, surrounded by a host dielectric medium. This surrounding material has been chosen to be selectively lossy only in one quadrant of the cross (Figure 1e). For simulations, the particles were distributed in an ordered array with 600 nm periodicity. The particle dimensions (marked in Figure 1e) were taken to be $w = 100$ nm, $t = 20$ nm, and $l = 400$ nm. The refractive index of the substrate, as well as embedding dielectric are subject to changes. A Drude model fit for gold was chosen for the particle's material.³¹ The numerical modeling has been performed in the frequency domain using the commercial software CST Microwave Studio with periodic boundary conditions. The polarization resolved spectra of transmission and reflection scattering parameters from the array have been modeled at normal incidence. The transmission scattering parameters are defined so that $T = |S_T|^2$. In our case, we define two transmission parameters depending on the relative orientation of the light polarization considered at the input and the output, given by $S_T^{\text{direct}} = (E_H^{\text{out}}/\eta_{\text{subs}}^{1/2})/(E_H^{\text{in}}/\eta_0^{1/2}) = (E_V^{\text{out}}/\eta_{\text{subs}}^{1/2})/(E_V^{\text{in}}/\eta_0^{1/2})$ and $S_T^{\text{cross}} = (E_H^{\text{out}}/\eta_{\text{subs}}^{1/2})/(E_V^{\text{in}}/\eta_0^{1/2}) = (E_V^{\text{out}}/\eta_{\text{subs}}^{1/2})/(E_H^{\text{in}}/\eta_0^{1/2})$ corresponding to the transmission of light with the same and orthogonal polarization, respectively. E_V and E_H are the vertical and horizontal electric fields, respectively, and η_{subs} and η_0 are the characteristic impedances of the substrate and vacuum. Since the scattering parameters are proportional to the electric field, the ratio of S_T^{cross} and S_T^{direct} is equal to the ratio of orthogonal polarization amplitudes at the output.

AUTHOR INFORMATION

Corresponding Author

*E-mail: pavel.ginzburg@kcl.ac.uk.

Author Contributions

§These authors contributed equally.

Notes

The authors declare no competing financial interest.

ACKNOWLEDGMENTS

This work has been supported in part by EPSRC (UK). P.G. acknowledges Royal Society for a Newton International Fellowship. F.J.R.-F. acknowledges support from grant FPI of GV and the Spanish MICINN under contracts CONSOLIDER EMET CSD2008-00066 and TEC2011-28664-C02-02.

REFERENCES

- (1) Hanle, W. Über Magnetische Beeinflussung Der Polarisation Der Resonanzfluoreszenz. *Z. Phys. A-Hadron. Nucl.* **1924**, *30*, 93–105.
- (2) Colegrove, F.; Franken, P.; Lewis, R.; Sands, R. Novel Method of Spectroscopy With Applications to Precision Fine Structure Measurements. *Phys. Rev. Lett.* **1959**, *3*, 420–422.
- (3) Stenflo, J. O. The Hanle Effect and the Diagnostics of Turbulent Magnetic Fields in the Solar Atmosphere. *Sol. Phys.* **1982**, *80*, 209–226.
- (4) Ignace, R.; Nordsieck, K. H.; Cassinelli, J. P. The Hanle Effect as a Diagnostic of Magnetic Fields in Stellar Envelopes. I. Theoretical Results for Integrated Line Profiles. *Astrophys. J.* **1997**, *486*, 550–570.
- (5) Labeyrie, G.; Miniatura, C.; Müller, C.; Sigwarth, O.; Delande, D.; Kaiser, R. Hanle Effect in Coherent Backscattering. *Phys. Rev. Lett.* **2002**, *89*, 163901.
- (6) MacKintosh, F.; John, S. Coherent Backscattering of Light in the Presence of Time-reversal-noninvariant and Parity-nonconserving Media. *Phys. Rev. B* **1988**, *37*, 1884–1897.
- (7) Luk'yanchuk, B.; Zheludev, N. I.; Maier, S. A.; Halas, N. J.; Nordlander, P.; Giessen, H.; Chong, C. T. The Fano Resonance in Plasmonic Nanostructures and Metamaterials. *Nat. Mater.* **2010**, *9*, 707–715.
- (8) Liu, N.; Langguth, L.; Weiss, T.; Kästel, J.; Fleischhauer, M.; Pfau, T.; Giessen, H. Plasmonic Analogue of Electromagnetically Induced Transparency at the Drude Damping Limit. *Nat. Mater.* **2009**, *8*, 758–762.
- (9) Moiseyev, N. *Non-Hermitian Quantum Mechanics*; Cambridge University Press: New York, 2011.
- (10) Bender, C. M. Making Sense of non-Hermitian Hamiltonians. *Rep. Prog. Phys.* **2007**, *70*, 947–1018.
- (11) Berkovitch, N.; Ginzburg, P.; Orenstein, M. Concave Plasmonic Particles: Broad-band Geometrical Tunability in the Near-infrared. *Nano Lett.* **2010**, *10*, 1405–1408.
- (12) Prodan, E.; Radloff, C.; Halas, N. J.; Nordlander, P. A Hybridization Model for the Plasmon Response of Complex Nanostructures. *Science* **2003**, *302*, 419–422.
- (13) Berkovitch, N.; Ginzburg, P.; Orenstein, M. Nano-plasmonic Antennas in the Near Infrared Regime. *J. Phys.: Condens. Matter* **2012**, *24*, 073202.
- (14) Ginzburg, P.; Berkovitch, N.; Nevet, A.; Shor, I.; Orenstein, M. Resonances On-demand for Plasmonic Nano-particles. *Nano Lett.* **2011**, *11*, 2329–2333.
- (15) Gilary, I.; Kaprálová-Žďánská, P.; Moiseyev, N. Ab Initio Calculation of Harmonic Generation Spectra of Helium Using a Time-dependent non-Hermitian Formalism. *Phys. Rev. A* **2006**, *74*, 052505.
- (16) Ginzburg, P.; Hayat, A.; Vishnyakov, V.; Orenstein, M. Photonic Logic by Linear Unidirectional Interference. *Opt. Express* **2009**, *17*, 4251–4256.
- (17) Joannopoulos, J. D.; Johnson, S. G.; Winn, J. N.; Meade, R. D. *Photonic Crystals: Molding the Flow of Light*; Princeton University Press: Princeton, NJ, 2008.
- (18) Asplund, C.; Mogg, S.; Plaine, G.; Salomonsson, F.; Chitica, N.; Hammar, M. Doping-induced Losses in AlAs/GaAs Distributed Bragg Reflectors. *J. Appl. Phys.* **2001**, *90*, 794–800.
- (19) Eldada, L.; Shacklette, L. W. Advances in Polymer Integrated Optics. *IEEE J. Sel. Topics Quantum Electron.* **2000**, *6*, 54–68.
- (20) Papakostas, A.; Potts, A.; Bagnall, D.; Prosvirnin, S.; Coles, H.; Zheludev, N. Optical Manifestations of Planar Chirality. *Phys. Rev. Lett.* **2003**, *90*, 107404.
- (21) Elliott, J.; Smolyaninov, I. I.; Zheludev, N. I.; Zayats, A. V. Polarization Control of Optical Transmission of a Periodic Array of Elliptical Nanoholes in a Metal Film. *Opt. Lett.* **2004**, *29*, 1414–1416.
- (22) Elliott, J.; Smolyaninov, I.; Zheludev, N.; Zayats, A. Wavelength Dependent Birefringence of Surface Plasmon Polaritonic Crystals. *Phys. Rev. B* **2004**, *70*, 233403.
- (23) Drezet, A.; Genet, C.; Laluet, J.-Y.; Ebbesen, T. W. Optical Chirality Without Optical Activity: How Surface Plasmons Give a Twist to Light. *Opt. Express* **2008**, *16*, 12559–12570.

- (24) Zhao, Y.; Alù, A. Manipulating Light Polarization with Ultrathin Plasmonic Metasurfaces. *Phys. Rev. B* **2011**, *84*, 205428.
- (25) Gansel, J. K.; Thiel, M.; Rill, M. S.; Decker, M.; Bade, K.; Saile, V.; von Freymann, G.; Linden, S.; Wegener, M. Gold Helix Photonic Metamaterial as Broadband Circular Polarizer. *Science* **2009**, *325*, 1513–1515.
- (26) Gansel, J. K.; Latzel, M.; Frölich, A.; Kaschke, J.; Thiel, M.; Wegener, M. Tapered Gold-helix Metamaterials as Improved Circular Polarizers. *Appl. Phys. Lett.* **2012**, *100*, 101109.
- (27) Engheta, N. Circuits with Light at Nanoscales: Optical Nanocircuits Inspired by Metamaterials. *Science* **2007**, *317*, 1698–1702.
- (28) Ni, X.; Emani, N. K.; Kildishev, A. V.; Boltasseva, A.; Shalaev, V. M. Broadband Light Bending with Plasmonic Nanoantennas. *Science* **2012**, *335*, 427.
- (29) Yu, N.; Genevet, P.; Kats, M. A.; Aieta, F.; Tetienne, J.-P.; Capasso, F.; Gaburro, Z. Light Propagation with Phase Discontinuities: Generalized Laws of Reflection and Refraction. *Science* **2011**, *334*, 333–337.
- (30) Quidant, R.; Kreuzer, M. Biosensing: Plasmons Offer a Helping Hand. *Nat. Nanotechnol.* **2010**, *5*, 762–763.
- (31) Johnson, P. B.; Christy, R. W. Optical Constants of the Noble Metals. *Phys. Rev. B* **1972**, *6*, 4370–4379.